Nonleptonic charmed-meson decays

Sinan Kaptanoğlu *
Stanford Linear Accelerator Center, Stanford University, Stanford, California 94305
(Received 23 March 1978)

In this paper we compute and interrelate various nonleptonic charmed-meson decay matrix elements. With the assumption that the decay Hamiltonian is in the $\Delta I = 1$ form, numerous decay rates are interrelated. The predictions are compared to the experiment whenever sufficient data is available. In other cases we compare our results to those of the statistical model of Quigg and Rosner. To estimate the value of the $D \to \bar{K}\pi\pi$ decay amplitudes we make use of PCAC (partial conservation of axial-vector current) and we attribute the enhancement of these amplitudes relative to $D \to \bar{K}\pi$ amplitudes to the final-state interactions. We suggest an approximate treatment of the problem and show that even though the parameter dependence is unavoidable it is possible to obtain the desired enhancement. Some numerical and graphical results are presented.

I. INTRODUCTION

A. Brief review of the current experimental status

The presently known charmed particles D^0 and D^+ have been discovered by the SLAC-LBL group as peaks in $\bar{K}\pi$, $\bar{K}\pi\pi$, and $\bar{K}\pi\pi\pi$ invariant masses coming from e^+e^- annihilation.[1] Evidence for the charmed strange meson F^+ is accumulating, but it is not yet conclusive.[2]

Experimentally, $D^0 \to K^-\pi^+$, $D^0 \to \bar{K}^0\pi^+\pi^-$, $D^0 \to K^-\pi^+\pi^+\pi^-$, $D^+ \to \bar{K}^0\pi^+$, and $D^+ \to K^-\pi^+\pi^+$ are the only established decay modes of D^0 and D^+.[3] It is also known that the leptonic and semileptonic decays occur about 10% to 20% of the time, but the exact decay modes have not yet been determined.[4]

In an analysis carried out by the SLAC-LBL group consistency of the data with the spin-0 assignment is reported.[5] The same analysis also confirmed the spin-1 assignment for the D^{0*} and D^{+*}. The study of the Dalitz plot by the same group has shown that the spin-parity of the final state in $D^+ \to K^-\pi^+\pi^+$ decay is not compatible with $J^P = 1^-$ or 2^+. On the other hand, clearly, three pseudoscalars cannot be in $J^P = 0^+$. Since $D^+ \to \bar{K}^0\pi^+$ decay has a final state of spin-parity $0^+, 1^-, 2^+, \ldots$ it is obvious that unless D is of spin 3 or higher, the existence of both modes $D^+ \to \bar{K}^0\pi^+$, $D^+ \to K^-\pi^+\pi^+$ implies parity violation, and establishes that the decay must be weak. The corresponding analysis of the Dalitz plot for the $D^0 \to \bar{K}^0\pi^+\pi^-$ decay has not yet been done, but the most reasonable assumption that D^+ and D^0 are isodoublets would suffice to extend the same conclusion to D^0 decays as well.

The question of $\bar{D}^0 - D^0$ mixing has not been settled yet. If one assumes that the fourth flavor carried by D^0 and D^+ is the same flavor originally conjectured by Bjorken and Glashow, one expects that $D^+ \to K^-\pi^+\pi^+$ should go but $D^+ \to K^+\pi^+\pi^-$ must be forbidden.[6] Furthermore the decays that do not involve a $\bar{K}$ must be suppressed by the Cabibbo angle. The experimental evidence supports both of these predictions, and limits the possible weak $\bar{D}^0 - D^0$ mixing to be small; however, the data are not very accurate and conclusive yet.[2]

The analysis of the Dalitz plots has also established that the $\bar{K}^*\pi$ and $\bar{K}\rho$ contributions to the $\bar{K}\pi\pi$ final state are negligible.[7] In the Dalitz plots no other intermediate resonant states are observed. The present data are not sufficient to determine the variation in the Dalitz plot accurately, but the obvious feature is that such a variation must be fairly smooth.

Even though the parity violation is well established, the present data, including the leptonic or semileptonic decays, is insufficient to determine the form of the interaction. It is consistent with $V-A$, but not good enough to rule out other possibilities.

The final piece of experimental evidence relevant to our paper is the enhancement of the three- and four-body nonleptonic final states over the two-body nonleptonic final states. As given by G. J. Feldman, the relative decay rates are listed in Table I.[8]

B. The method

In this paper we will attempt to interrelate various nonleptonic low-multiplicity decays of the charmed mesons.

Because the Dalitz plots seem to be fairly smooth, the simple assumption that the decay matrix element is constant over the Dalitz plot is naturally the first thing to try. This matrix element was first estimated by Gaillard, Lee, and Rosner,[9] Jackson,[10] and Quigg and Rosner,[11] based on a simple statistical model. As the mass

TABLE I. σB in nb for various D decay modes at three values of $E_{c.m.}$.

Mode \ $E_{c.m.}$ (GeV)	3.774	4.028	4.414
$D^0 \to K^{\mp}\pi^{\pm}$	0.27 ± 0.05	0.57 ± 0.11	0.30 ± 0.09
$\bar{K}^0\pi^+\pi^- + \text{c.c.}$	0.44 ± 0.11	1.09 ± 0.30	0.91 ± 0.34
$K^{\mp}\pi^{\pm}\pi^+\pi^-$	0.34 ± 0.09	0.83 ± 0.27	0.91 ± 0.39
$\pi^+\pi^-$	···	<0.04	···
K^+K^-	···	<0.04	···
Total D^0 observed modes	1.15 ± 0.15	2.49 ± 0.42	2.42 ± 0.53
$D^+ \to \bar{K}^0\pi^+ + \text{c.c.}$	0.15 ± 0.05	<0.18	···
$K^{\mp}\pi^{\pm}\pi^{\pm}$	0.34 ± 0.05	0.40 ± 0.10	0.33 ± 0.12
$\pi^{\pm}\pi^+\pi^-$	···	0.03	···

Mode	Branching fraction (%)
$D^0 \to K^-\pi^+$	2.2 ± 0.6
$\bar{K}^0\pi^+\pi^-$	3.5 ± 1.1
$K^-\pi^+\pi^-\pi^+$	2.7 ± 0.9
$D^+ \to \bar{K}^0\pi^+$	1.5 ± 0.6
$K^-\pi^+\pi^+$	3.5 ± 0.9

of the D particle approaches infinity, and as the multiplicity of the final state grows ($N > 4$), their approach may be the best approximation. Nevertheless since the D mass is not all that high, their predictions for low multiplicities ($N \lesssim 4$) may not be correct. In this paper we will follow an alternate method for the two- and three-body final states using the standard Lehmann-Symanzik-Zimmermann (LSZ) reduction technique and the hypothesis of partically conserved axial-vector current (PCAC).

One may object that the success of the PCAC hypothesis is limited to low-energy phenomena, and yet, in the decay of D particles, the final products are fairly energetic. However, PCAC need not be interpreted as an approximation to physics for zero momentum. Alternately, we can assume that PCAC is an exact operator equation between the pseudoscalar field and the divergence of the axial-vector current. In this case, all the results obtained by the application of this hypothesis to the standard reduction of scalar matrix elements must be interpreted as exact results. However, the actual computation can only be carried out for zero momentum, which lies outside the physical region. We will call these zero-momentum points the PCAC points. The task is then to extrapolate the matrix element computed at the PCAC points to the physical region. There is no proven and universally accepted way of doing this, and without approximations and plausibility arguments the task may be impossible. For low-energy phenomena, of course, the matrix element has to be extrapolated to a small nearby region for which a simple linear approximation may work very well, as was the case with $K \to \pi\pi\pi$ decays.[12]

Such a linear approximation is again the first thing to try even though for the decay of D particles it is not expected to produce correct results considering the range of extrapolation. The actual calculations showed that the result is about four times smaller in amplitude than the experimental value. To extrapolate the matrix element to the physical region more realistically, the final-state interactions must be included. As will be shown in Sec. II it is possible to employ the final-state interactions to obtain the desired enhancement of the matrix element over the physical region without introducing any resonant intermediate states, which seem to be absent experimentally.

In this paper actual numerical results will be obtained for various decays, and wherever the experimental data is available the comparison will be made. Owing to the lack of sufficient data for most of the decays that has one or more π^0 in the final state, comparison with experiment will not be possible for most of the predicted decay modes. For these cases we will compare our results to that of Quigg and Rosner. For several particular decay ratios our prediction will be different by more than 100%.

At the end we provide two appendixes. The first one is for the computation of the matrix elements in detail, the next one is for the computation of the Omnes functions relevant to our problem.[13] Most of the numerical part of the work for this paper was done on the IBM/370 computer at SLAC. The numerical integrations were carried out by the use of the Fortran integration routine SHEP.

II. MATRIX ELEMENTS FOR D AND F DECAYS

A. General assumptions

In the rest of this paper we will assume that the charm selection rule $\Delta S = \Delta C$ holds for all weak charm decays, and $\bar{D}^0 - D^0$ mixing is small or vanishing. As mentioned in the Introduction, the experimental evidence for this assumption is good but not conclusive. We will further assume that D^0 and D^+ form an isospin doublet and both are assigned $J^P = 0^-$ spin-parity. We will also assume that

$$[Q_a + Q_a^5, H_w(0)] = 0\,, \tag{1}$$

where H_w is the weak Hamiltonian density, and Q_a and Q_a^5 are the weak scalar and pseudoscalar charges associated with the vector and axial-vector currents, respectively. The subscript a is the group index. For most purposes this

assumption is equivalent to the $V-A$ form of the interaction Hamiltonian. The PCAC hypothesis will be stated as

$$\partial_\mu A_a^\mu(x) = f_{(a)} m_{(a)}{}^2 \phi_{(a)}(x) \tag{2}$$

where μ is the Lorentz index, A_a^μ is the axial-vector current, and the pseudoscalar field, where $m_{(a)}$ is its mass and $f_{(a)}$ is the decay constant defined by

$$(0|A_a^\mu(0)|\phi_b(p)) = i\delta_{ab} p^\mu f_{(b)} .$$

We will also assume that the final pseudoscalars in the D decays are all in relative $L=0$ states of orbital angular momentum. Owing to the angular momentum barrier, we expect this assumtpion to be true in the majority of the decays. The lack of $\bar{K}^*\pi$ and $\bar{K}\rho$ final states supports our assumption. We must mention that there is evidence that $D \to \bar{K}\rho\pi$ decay may be the dominant $\bar{K}\pi\pi\pi$ source.[7] The application of the standard reduction technique and PCAC will then imply the existence of $D \to \bar{K}\rho$ decay, which is very suppressed. A possible explanation is to assume that $\rho\pi$ in the final state come from the decay of a more massive particle. Experimentally, A_2 is ruled out to a good confidence level, but A_1 and others may account for the data.[7] We emphasize, however, that the s-wave approximation is probably the weakest of all our assumptions. It is conceivable that some unknown dynamical mechanism may enhance the higher partial amplitudes.

With the above assumption then, whenever applicable we will symmetrise the final state with respect to all the pions in it, since the pions must be in relative $I=0,2$ isospin states and not in $I=1$. Some of our results will crucially depend on this symmetrization, and if for some reason the p waves are enhanced, some of the relative decay rates we obtained may change drastically.

B. Reduction of the three-body matrix element

Define

$$\mathfrak{M}^{ijl}(k_1,k_2,k_3;q) \equiv (\pi^i(k_1)\pi^j(k_2)\pi^l(k_3)|H_w(0)|D(p)),$$

where i, j, and l are group [SU(3)] indices, and $q = p - k_1 - k_2 - k_3$, which we allow to be nonzero until the end. The standard LSZ reduction yields

$$\mathfrak{M}^{ijl}(k_1,k_2,k_3;q) = -i(k_3{}^2 - m_{(l)}{}^2)\int d^4x e^{ik_3\cdot x}(\pi^i(k_1)\pi^j(k_2)|T[\phi_l(x)H_w(0)]|D(p))$$

which with the help of PCAC becomes

$$\mathfrak{M}^{ijl}(k_1,k_2,k_3;q) = \frac{i(k_3{}^2 - m_{(l)}{}^2)}{f_{(l)} m_{(l)}{}^2}\Big\{(\pi^i(k_1)\pi^j(k_2)|[Q_l{}^5(0), H_w(0)]|D(p)) + ik_3^\mu\int d^4x\, e^{ik_3\cdot x}(\pi^i(k_1)\pi^j(k_2)|T[A_\mu{}^l(x)H_w(0)]|D(p) + \text{possible Schwinger terms}\cdots\Big\}.$$

The reason for writing this equation in full is to emphasize that we consider it exact. Then we take the $k_3 \to 0$ limit and use Eq. (1) to get

$$\mathfrak{M}^{ijl}(k_1,k_2,0;q) = \frac{i}{f_{(l)}}(\pi^i(k_1)\pi^j(k_2)|[Q^l, H_w(0)]|D(p)). \tag{3}$$

The individual matrix elements for each one of the possible five decays of D^+ and D^0 are given by Eq. (A1) in Appendix A.

Because we assume that the pions are in $I=0,2$ isospin states, we have to symmetrize the matrix element with respect to the final pions. Then we define the symmetrized matrix elements $\mathfrak{N}$ as

$$\mathfrak{N}(k_1,k_2,k_3;q) = \begin{cases} \mathfrak{M}(k_1,k_2,k_3;q) \text{ if the pions are identical.} \\ [\mathfrak{M}(k_1,k_2,k_3;q) + \mathfrak{M}(k_1,k_2,k_3;q)]/\sqrt{2} \text{ otherwise.} \end{cases}$$

Since the pions are treated symmetrically, taking both of them out of the matrix element and letting their momenta go to zero will not produce any nontrivial relations because we can take $m_\pi{}^2 \approx 0$. This point will be clearly explained in the next section. Again, a full account of the PCAC relations when both pions are taken out of the matrix element is given in Appendix A.

Even though the kaon PCAC relations are not considered as reliable as those of pions, the case for which the kaon is taken out of the matrix element is also worked out in Appendix A. At the end, we will make use of these as well as the pion PCAC relations.

The equations (A2) and (A4) in Appendix A are particularly important. They state that

$$\mathfrak{M}^{++}(k_1, k_2, 0; q) = -\sqrt{2}\,\mathfrak{M}^{0+-}(k_1, k_2, 0; q)\,. \tag{4}$$

If we make the roughest assumption now, that the value of the matrix element computed at the pion PCAC points is approximately equal to the value of the matrix element over the actual Dalitz plot, using Eq. (4) we reach the following two conclusions, both of which are in disagreement with experiment.

The first prediction is that the $D^+ \to K^-\pi^+\pi^+$ rate must be twice as large as that of $D^0 \to \bar{K}^0\pi^+\pi^-$. The experimental number is clearly not 2 but about 0.85 ± 0.30.[8] Secondly we predict that the ratio of the $D^0 \to \bar{K}^0\pi^+\pi^-$ rate to that of $D^0 \to K^-\pi^+$ must be less than 0.4 compared to the experimental value 1.75 ± 0.70.[8] It is clear, therefore, that some mechanism of enhancement is needed.

The simplest way of achieving such an enhancement is by means of one or more intermediate resonant states. Experimental evidence, however, clearly negates this possibility. On the other hand, the final-state interactions can conceivably produce such an enhancement without going through a resonance. Unfortunately, there is no unique, relativistic formulation of the final-state interactions for three particles. We will assume the following simple approximate form for the matrix element:

$$\mathfrak{M}(k_1, k_2, k_3; q) \approx R^{\pi}_{\bar{K}\pi}(s_{12}, t_3) + R^{\pi}_{\bar{K}\pi}(s_{13}, t_2) + R^{\bar{K}}_{\pi\pi}(s_{23}, t_1)\,, \tag{5}$$

where the R amplitudes will be separated to their isospin parts $R^{I_2}_{I_1}$, I_1 being the total isospin of the lower two particles and I_2 being the isospin of the $\bar{K}\pi\pi$ system, and $s_{ij} = (k_i + k_j)^2$ for $i \neq j$, and $t_i = q \cdot k_i$, $i, j = 1, 2, 3$. Each amplitude R has the form

$$R^{I_2}_{I_1}(s, t) = N^{I_2}_{I_1}(s, t)/D_{I_1}(s)\,, \tag{6}$$

where the numerator is presumably a smooth function of s and t, and the denominator is the corresponding Omnés function (see Appendix B). This form of the amplitude is not strictly correct. Above all, it violates unitarity. However, in various situations it provides a fair approximation to the actual scattering amplitude, and it is the only form that is easy to manipulate without trying to solve several coupled integro-differential equations.[13] In the actual application to our problem we will approximate the numerator as a simple linear polynomial, and hope that it provides a reasonable approximation over the energy range we are concerned with. The coefficients of the linear polynomials for each different amplitude will be treated as unknowns to be determined by the value of the amplitude computed at PCAC points.

Unfortunately, as it stands, the problem cannot be solved without additional assumptions. Assuming that the Hamiltonian takes the most general form introduces too many amplitudes (hence too many coefficients to be determined in the numerator). At this point we found it impossible to continue without introducing the extra assumption that the Hamiltonian is mainly of the $\Delta I = 1$, $\Delta I_3 = 1$ type; the $\Delta I = 2$, $\Delta I_3 = 1$ part of it is either very small or vanishing.

This is not an *ad hoc* assumption at all. It can be justified by the current-current form of the Hamiltonian.

If the Hamiltonian density is of the current-current form, the $\Delta I = 2$ part of the Hamiltonian vanishes identically. The current-current form of the Hamiltonian may not be strictly correct; nevertheless, in a lot of cases we know that it provides a good approximation. We also have to emphasize that the $\Delta I = 2$ part of the Hamiltonian may be negligible even if the form of the Hamiltonian is not current-current type. PCAC itself is very suggestive for the $\Delta I = 1$ assumption (see Appendix A).

We use the $\Delta I = 1$ hypothesis to write

$$[I^+, H_w(0)] = 0\,. \tag{7}$$

By manipulating the isospin raising and lowering operators we get

$$(\bar{K}^0\pi^+ | H_w | D^+) = -(\bar{K}^0\pi^+ | [H_w, I^+] | D^0) + (K^-\pi^+ | H_w | D^0) + \sqrt{2}\,(\bar{K}^0\pi^0 | H_w | D^0)$$

which implies then

$$T^{0+} - T^{-+} - \sqrt{2}\,T^{00} = 0\,, \tag{8}$$

where the notation refers to the charges of the final particles starting with the charge of $\bar{K}$ [see Eq. (A1) in Appendix A].

Having limited the form of the amplitude we can proceed immediately to compute the $D \to \bar{K}\pi\pi$ matrix elements. However, we would like to postpone this for a while and study the immediate consequences of the $\Delta I = I$ assumption. As we will see, this one turns out to be a very powerful assumption in its predictive power.

C. Immediate consequences of $\Delta I = 1$ assumption

In the following section we treat $(K^-, \bar{K}^0)$ and (D^0, D^+) as isospin antidoublets rather than doublets. This way our phase convention matches that of standard SU(N). The same convention also requires that (π^-, π^0, π^+) be an isotriplet with the following signs for the raising and lowering operators:

$$I^- | \pi^+ \rangle = -\sqrt{2}\,| \pi^0 \rangle,$$

$$I^-|\pi^0) = \sqrt{2}\,|\pi^-),$$
$$I^+|\pi^-) = \sqrt{2}\,|\pi^0),$$

and

$$I^+|\pi^0) = -\sqrt{2}\,|\pi^+).$$

For the group SU(2) alone, admittedly, this is a highly unorthodox convention because a doublet is unitarily equivalent to an antidoublet; however, it is easier to manipulate when extensions to SU(3) and SU(4) are made, for which N-plets and anti-N-plets are no longer equivalent.

(i) Starting from

$$(\bar{K}^0\pi^+\pi^+|H_w I^+|D^+) = 0$$

and manipulating the $I^\pm$ operators and using Eq. (7), we get

$$0 = -\sqrt{2}\,[(\bar{K}^0\pi^+\pi^0|H_w|D^+) + (\bar{K}^0\pi^0\pi^+|H_w|D^+)] - (K^-\pi^+\pi^+|H_w|D^+),$$

which implies

$$\mathfrak{M}^{0+0}(k_1,k_2,k_3;q) = -\tfrac{1}{2}\,\mathfrak{M}^{-++}(k_1,k_2,k_3;q), \tag{9}$$

where the amplitude is symmetrized with respect to both the pions and labeled by the charges of the final particles starting from $\bar{K}$.

The manipulation of $I^\pm$ operators with other amplitudes immediately produces two more similar relations

$$\mathfrak{M}^{-+0}(k_1,k_2,k_3;q) = \tfrac{1}{2}\,\mathfrak{M}^{-++}(k_1,k_2,k_3;q), \tag{10}$$

$$\mathfrak{M}^{000}(k_1,k_2,k_3;q) = \tfrac{1}{2}[\sqrt{2}\,\mathfrak{M}^{0+-}(k_1,k_2,k_3;q) - \mathfrak{M}^{-++}(k_1,k_2,k_3;q)]. \tag{11}$$

We no longer have five different amplitudes; we can express the three amplitudes containing a final π^0 in terms of the other two.

(ii) We can use the same method for the four-particle final states as well. There are seven $D\to\bar{K}\pi\pi\pi$ decays, five of which can be eliminated in terms of only two of them. The results are

$$\begin{aligned}
&\mathfrak{M}^{-++0} = 0,\\
&\mathfrak{M}^{0+00} = \tfrac{1}{2}\,\mathfrak{M}^{0++-}\\
&\mathfrak{M}^{-+00} = \tfrac{1}{2}\,\mathfrak{M}^{-++-},\\
&\mathfrak{M}^{0+-0} = \tfrac{1}{2}\,(\mathfrak{M}^{0++-} - \mathfrak{M}^{-++-}),\\
&\mathfrak{M}^{0000} = \tfrac{1}{2}\,(\tfrac{3}{2})^{1/2}(\mathfrak{M}^{0++-} - \mathfrak{M}^{-++-}),
\end{aligned} \tag{12}$$

where again the labels in the amplitudes refer to the charges of the final particles starting from $\bar{K}$.

(iii) The application of this assumption and technique to the $D\to\bar{K}\eta\pi\pi$ decays gives

$$\mathfrak{M}^{0+}_{(\eta)} - \mathfrak{M}^{-+}_{(\eta)} = \sqrt{2}\,\mathfrak{M}^{00}_{(\eta)}, \tag{13}$$

with obvious notation.

(iv) Similar to the case of $D\to\bar{K}\pi\pi\pi$ decays, the application of the $\Delta I = 1$ hypothesis eliminates three of the five $D\to\bar{K}\eta\pi\pi\pi$ amplitudes in terms of two of them

$$\begin{aligned}
&\mathfrak{M}^{0+0}_{(\eta)} = -\tfrac{1}{2}\,\mathfrak{M}^{-++}_{(\eta)},\\
&\mathfrak{M}^{-+0}_{(\eta)} = \tfrac{1}{2}\,\mathfrak{M}^{-++}_{(\eta)}\\
&\mathfrak{M}^{000}_{(\eta)} = \tfrac{1}{2}\,(\sqrt{2}\,\mathfrak{M}^{0+-}_{(\eta)} - \mathfrak{M}^{-++}_{(\eta)}).
\end{aligned} \tag{14}$$

(v) $F^+\to\bar{K}(n\pi)$ decays are Cabibbo-angle-suppressed, and we do not discuss them here. $F^+\to\pi^+\pi^0$ is not allowed by isospin. Thus we start with $F\to\pi\pi\pi$ for the F decays. In this case, starting from

$$(\pi^+\pi^+\pi^0|HI^+|F^+) = 0,$$

we obtain

$$\mathfrak{M}_{F^+\to\pi^+\pi^+\pi^-} = 2\,\mathfrak{M}_{F^+\to\pi^+\pi^0\pi^0}. \tag{15}$$

The two $F\to\pi\pi\pi\pi$ decays can be related similarly

$$\sqrt{3}\,\mathfrak{M}_{F^+\to\pi^+\pi^0\pi^0\pi^0} = \mathfrak{M}_{F^+\to\pi^+\pi^+\pi^0\pi^-} = 0, \tag{16}$$

where, to get the correct factor, symmetrization with respect to all pions was carried out. Note that the above decays have to vanish as s-wave amplitudes, but they can proceed through p-wave or higher channels.

(vi) For the three possible $F\to K\bar{K}\pi$, we find the relation

$$(K^0\bar{K}^0\pi^+|H_w|F^+) = (K^+K^-\pi^+|H_w|F^+) + \sqrt{2}\,(K^+\bar{K}^0\pi^0|H_w|F^+), \tag{17}$$

and for the five allowed $F\to K\bar{K}\pi\pi$ decays we get

$$\begin{aligned}
&\mathfrak{M}^{00+0} = -\tfrac{1}{2}\,\mathfrak{M}^{0-++},\\
&\mathfrak{M}^{-+0} = \tfrac{1}{2}\,\mathfrak{M}^{0-++},\\
&\mathfrak{M}^{+000} = \tfrac{1}{2}(\sqrt{2}\,\mathfrak{M}^{+0+-} - \mathfrak{M}^{0-++}),
\end{aligned} \tag{18}$$

where now the labels of the amplitudes refer to the charges starting from K, then followed by $\bar{K}$ and pions.

(vii) The two possible $F\to\eta\pi\pi\pi$ decays are of course related the same way as the $F\to\pi\pi\pi$ decays:

$$\mathfrak{M}_{F^+\to\eta\pi^+\pi^+\pi^-} = 2\,\mathfrak{M}_{F^+\to\eta\pi^+\pi^0\pi^0}. \tag{19}$$

At present, experimental data are not available to check most of these predictions. Various decay ratios are summarized in Table II.

We can compare some of our predictions to those of Quigg and Rosner based on the statistical model.[11]

(i) We predict that the $D^+\to K^-\pi^+\pi^+$ rate will be 4 times larger than the $D^+\to\bar{K}^0\pi^+\pi^0$ rate. Quigg and Rosner predict a ratio of about 65%.

TABLE II. The constraints on various amplitudes imposed by the $\Delta I = 1$ hypothesis.

Decay mode	Decay rate
$D^0 \to K^- \pi^+$	$\lvert a_1 \rvert^2$
$D^+ \to \bar{K}^0 \pi^+$	$\lvert b_1 \rvert^2$
$D^0 \to \bar{K}^0 \pi^0$	$\lvert a_1 - b_1 \rvert^2/2$
$D^0 \to \bar{K}^0 \pi^+ \pi^-$	$\lvert a_2 \rvert^2$
$D^+ \to K^- \pi^+ \pi^+$	$\lvert b_2 \rvert^2$
$D^+ \to \bar{K}^0 \pi^+ \pi^0$	$\lvert b_2 \rvert^2/4$
$D^0 \to K^- \pi^+ \pi^0$	$\lvert b_2 \rvert^2/4$
$D^0 \to \bar{K}^0 \pi^0 \pi^0$	$\lvert \sqrt{2}\, a_2 - b_2 \rvert^2/4$
$D^0 \to K^- \pi^+ \eta$	$\lvert a_3 \rvert^2$
$D^+ \to \bar{K}^0 \pi^+ \eta$	$\lvert b_3 \rvert^2$
$D^0 \to \bar{K}^0 \pi^0 \eta$	$\lvert a_3 - b_3 \rvert^2/2$
$D^+ \to K^- \pi^+ \pi^+ \pi^0$	0
$D^0 \to K^- \pi^+ \pi^+ \pi^-$	$\lvert a_4 \rvert^2$
$D^+ \to \bar{K}^0 \pi^+ \pi^+ \pi^-$	$\lvert b_4 \rvert^2$
$D^+ \to \bar{K}^0 \pi^+ \pi^0 \pi^0$	$\lvert b_4 \rvert^2/4$
$D^0 \to K^- \pi^+ \pi^0 \pi^0$	$\lvert b_4 \rvert^2/4$
$D^0 \to \bar{K}^0 \pi^+ \pi^- \pi^0$	$\lvert a_4 - b_4 \rvert^2/4$
$D^0 \to \bar{K}^0 \pi^0 \pi^0 \pi^0$	$3\lvert a_4 - b_4 \rvert^2/8$
$F^+ \to \pi^+ \pi^0$	0
$F^+ \to \pi^+ \pi^+ \pi^-$	$\lvert c_1 \rvert^2$
$F^+ \to \pi^+ \pi^0 \pi^0$	$\lvert c_1 \rvert^2/4$
$F^+ \to K^+ K^- \pi^+$	$\lvert c_2 \rvert^2$
$F^+ \to K^0 \bar{K}^0 \pi^+$	$\lvert d_2 \rvert^2$
$F^+ \to K^+ \bar{K}^0 \pi^0$	$\lvert c_2 - d_2 \rvert^2/2$
$F^+ \to \pi^+ \pi^+ \pi^0 \pi^-$	0
$F^+ \to \pi^+ \pi^0 \pi^0 \pi^0$	0
$F^+ \to \pi^+ \pi^+ \pi^- \eta$	$\lvert c_3 \rvert^2$
$F^+ \to \pi^+ \pi^0 \pi^0 \eta$	$\lvert c_3 \rvert^2/4$
$F^+ \to K^+ \bar{K}^0 \pi^+ \pi^-$	$\lvert c_4 \rvert^2$
$F^+ \to K^0 K^- \pi^+ \pi^+$	$\lvert d_4 \rvert^2$
$F^+ \to K^+ K^- \pi^+ \pi^0$	$\lvert d_4 \rvert^2/4$
$F^+ \to K^0 \bar{K}^0 \pi^+ \pi^0$	$\lvert d_4 \rvert^2/4$
$F^+ \to K^+ \bar{K}^0 \pi^0 \pi^0$	$\lvert \sqrt{2}\, c_4 - d_4 \rvert^2/4$

(ii) We predict that the $D^0 \to K^- \pi^+ \pi^0$ rate will be 4 times smaller than the $D^+ \to K^- \pi^+ \pi^+$ rate. The experimental branching ratio for the $D^0 \to K^- \pi^+ \pi^0$ decay is too high [$(12 \pm 6)\%$], but it is based on a small amount of data.[3] Considering the poor statistics and the fact that it is only 2 standard deviations away from anything else, we consider the possibility that, with better statistics, a lower rate for this decay will be established in the future experiments.

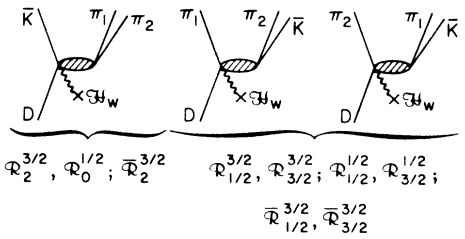

FIG. 1. Approximate form of the three-body amplitude assuming that the final particles interact two at a time, but not all three together.

(iii) We predict that the $D^+ \to K^- \pi^+ \pi^+ \pi^0$ decay rate must be much smaller than other $D \to \bar{K} \pi\pi\pi$ decays. This ratio in Quigg and Rosner's paper is of the order of 1. Also, similar to the previous case we estimate the rate for $D^+ \to \bar{K}^0 \pi^+ \pi^+ \pi^-$ to be 4 times as large as that of $D^+ \to \bar{K}^0 \pi^+ \pi^0 \pi^0$, where their prediction states a 1.3 times larger rate for the $D^+ \to \bar{K}^0 \pi^+ \pi^+ \pi^-$ decay.

(iv) In the case of F^+ decays, the ratio of the rates of $F^+ \to \pi^+ \pi^+ \pi^-$ and $F^+ \to \pi^+ \pi^0 \pi^0$ decays is 4, while Quigg and Rosner predict approximately 1.6. For the $F^+ \to \pi^+ \pi^+ \pi^0 \pi^-$ and $F^+ \to \pi^+ \pi^0 \pi^0 \pi^0$ decays we predict a vanishing rate, but their predictions for these channels are comparable to the other decay modes of F^+.

Clearly then, $F \to \pi\pi\pi\pi$ and $D^+ \to K^- \pi^+ \pi^+ \pi^0$ decays provide a very good test to see if and how much the p-wave and higher partial amplitudes are suppressed. A vanishing or small rate would support s-wave dominance, while a p-wave enhancement would allow these modes to have comparable rates to the other modes of decay.

D. $D \to \bar{K}\pi\pi$ matrix elements and the enhancement over the Dalitz plot

The $\Delta I = 1$ hypothesis eliminated three of the $D \to \bar{K}\pi\pi$ amplitudes that have one or more π^0 in the final state in terms of the experimentally observed decays $D^+ \to K^- \pi^+ \pi^+$ and $D^0 \to \bar{K}^0 \pi^+ \pi^-$. Therefore in this section we only worry about these two modes.

Equation (5) approximates the amplitude as the sum of three terms. Diagrammatically this can be represented as in Fig. 1. Now we can neglect the $\Delta I = 2$ contribution to the amplitudes, and separate the proper isospin parts to obtain

$$\mathfrak{A}^{-++}(k_1, k_2, k_3; q) = -(\tfrac{2}{3})^{1/2}[\bar{R}_{1/2}^{3/2}(s_{12}, t_3) + \bar{R}_{1/2}^{3/2}(s_{13}, t_2)] - (2/\sqrt{5})\bar{R}_2^{3/2}(s_{23}, t_1) - (\tfrac{2}{15})^{1/2}[\bar{R}_{3/2}^{3/2}(s_{12}, t_3) + \bar{R}_{3/2}^{3/2}(\bar{s}_{13}, t_2)], \tag{20}$$

$$\begin{aligned}\mathfrak{A}^{0+-}(k_1, k_2, k_3; q) = {} & \tfrac{1}{3}[R_{1/2}^{3/2}(s_{12}, t_3) + R_{1/2}^{3/2}(s_{13}, t_2)] + (\tfrac{2}{15})^{1/2} R_2^{3/2}(s_{23}, t_1) + (\sqrt{2}/3)[R_{1/2}^{1/2}(s_{12}, t_3) + R_{1/2}^{1/2}(s_{13}, t_2)] \\ & + (\tfrac{2}{3})^{1/2} R_0^{1/2}(s_{23}, t_1) \\ & + \tfrac{2}{3}[R_{3/2}^{1/2}(s_{12}, t_3) + R_{3/2}^{1/2}(s_{13}, t_2)] + (1/\sqrt{45})[R_{3/2}^{3/2}(s_{12}, t_3) + R_{3/2}^{3/2}(s_{13}, t_2)]. \end{aligned} \tag{21}$$

For the notation see Eq. (5) and (6). Note that $\bar{R}^{3/2}_{1/2} \neq R^{3/2}_{1/2}$, $\bar{R}^{3/2}_{3/2} \neq R^{3/2}_{3/2}$, and $\bar{R}^{2}_{3/2} \neq R^{2}_{3/2}$, but of course they are related. To find the relation, think of two (imaginary) intermediate states Y and U with $I=\frac{3}{2}$ and $I=\frac{1}{2}$, respectively, as shown diagrammatically in Fig. 2. We emphasize that we do not identify Y or U with any physical states. This must be considered no more than a gimmick to make it easy to picture the situation. Then we observe that

$$(Y^{+}|H_w|D^{+}) = -(Y^{+}|H_w I^{+}|D^{0}) = -\sqrt{3}(Y^{0}|H_w|D^{0}),$$

which gives us the desired relations

$$\bar{R}_{3/2}{}^{3/2}(s,t) = -\sqrt{3}\, R_{3/2}{}^{3/2}(s,t), \tag{22}$$

$$\bar{R}_{1/2}{}^{3/2}(s,t) = -\sqrt{3}\, R_{1/2}{}^{3/2}(s,t), \tag{23}$$

$$\bar{R}_{2}{}^{3/2}(s,t) = -\sqrt{3}\, R_{2}{}^{3/2}(s,t). \tag{24}$$

Now we are ready to impose the PCAC relations. We substitute Eqs. (20)–(24) into Eq. (4), and equate the parts with the same denominator (since the denominator is a known but arbitrary function of s_{ij}, only those parts of the amplitude with the same denominator, i.e., the same Omnès function, can add up to zero for all possible values of s_{ij}), and obtain

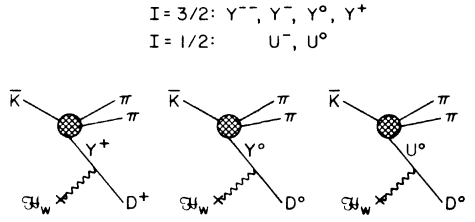

FIG. 2. Equations (22) through (24) can be deduced by assuming the reaction proceeds through the imaginary intermediate states Y and U.

$$R^{3/2}_{3/2}(s_{12},0) = -\frac{\sqrt{5}}{2} R^{1/2}_{3/2}(s_{12},0), \tag{25}$$

$$R^{3/2}_{1/2}(s_{12},0) = -\frac{1}{2\sqrt{2}} R^{1/2}_{1/2}(s_{12},0), \tag{26}$$

$$R^{1/2}_{0}(m_\pi{}^2,0) = -\frac{4}{\sqrt{5}} R^{3/2}_{2}(m_\pi{}^2,0). \tag{27}$$

We will not be interested in the matrix elements when the four-momentum is conserved, that is $q=0$. Substituting Eqs. (25) and (26) into (20) and (21) we obtain

$$\mathfrak{A}^{-++}(k_1,k_2,k_3;0) = \sqrt{2}\,[R^{3/2}_{1/2}(s_{12},0)+R^{3/2}_{1/2}(s_{13},0)] + 2\,(\tfrac{3}{5})^{1/2} R^{3/2}_{2}(s_{23},0) + (\tfrac{2}{5})^{1/2}[R^{3/2}_{3/2}(s_{12},0)+R^{3/2}_{3/2}(s_{13},0)], \tag{28}$$

$$\mathfrak{A}^{0+-}(k_1,k_2,k_3;0) = -[R^{3/2}_{1/2}(s_{12},0)+R^{3/2}_{1/2}(s_{13},0)] + (\tfrac{2}{15})^{1/2} R^{3/2}_{2}(s_{23},0) - \frac{1}{\sqrt{5}}[R^{3/2}_{3/2}(s_{12},0)+R^{3/2}_{3/2}(s_{13},0)] + (\tfrac{2}{5})^{1/2} R^{1/2}_{0}(s_{23},0). \tag{29}$$

Now note that the two PCAC conditions (A2) and (A4) in Appendix A are not independent, and they produce a single constraint

$$-(\tfrac{5}{2})^{1/2}\frac{i}{f_\pi} T^{00} = [R^{3/2}_{3/2}(m_D{}^2,0)+R^{3/2}_{3/2}(m_K{}^2,0)] + \sqrt{6}\, R^{3/2}_{2}(m_\pi{}^2,0) + \sqrt{5}\,[R^{3/2}_{1/2}(m_D{}^2,0)+R^{3/2}_{1/2}(m_K{}^2,0)]. \tag{30}$$

Also note that equation (A8) derived in Appendix A implies

$$R^{1/2}_{0}(0,0) = -\frac{4}{\sqrt{5}} R^{3/2}_{2}(0,0),$$

which we do not consider any different from Eq. (27). Our accuracy in this problem is far worse than $m_\pi{}^2/m_D{}^2$ and we have to take $m_\pi{}^2 \approx 0$. Therefore the PCAC relation when both pions are taken out of the matrix element simultaneously does not give us an extra constraint. Next we use the PCAC relations (A11) and (A12) derived for the kaons in Appendix A to get

$$R^{3/2}_{3/2}(m_K{}^2,0) + \sqrt{5}\, R^{3/2}_{1/2}(m_K{}^2,0) - \frac{1}{\sqrt{6}} R^{3/2}_{2}(m_D{}^2,0) - (\tfrac{5}{6})^{1/2} R^{1/2}_{0}(m_D{}^2,0) = -\frac{\sqrt{5}}{2}\frac{i}{f_K} T^{-+}, \tag{31}$$

$$R^{3/2}_{3/2}(m_K{}^2,0) + \sqrt{5}\, R^{3/2}_{1/2}(m_K{}^2,0) + \frac{1}{\sqrt{6}} R^{3/2}_{2}(m_D{}^2,0) - \tfrac{1}{2}(\tfrac{5}{6})^{1/2} R^{1/2}(m_D{}^2,0) = \tfrac{1}{2}(\tfrac{5}{2})^{1/2}\frac{i}{f_K} T^{00}. \tag{32}$$

As promised earlier we approximate the numerator function by a linear polynomial

$$\mathfrak{A}^{I_2}_{I_1}(s,0) \approx (a^{I_2}_{I_1} s + c^{I_2}_{I_1}),$$

and for the individual amplitudes we write

$$R^{I_2}_{I_1}(s,0) \approx \frac{a_{I_1} s + c_{I_1}}{D_{I_1}(s)},$$

where we suppressed the upper index, for we no longer need it. This way we see that we have eight coefficients to determine: a_0, c_0, $a_{1/2}$, $c_{1/2}$, $a_{3/2}$, $c_{3/2}$, a_2, and c_2, but we have only four equations [Eqs. (27), (30), (31), and (32)]. Unfor-

tunately, the problem is underdetermined.

Since the $I=\frac{3}{2}$ phase shift is approximately zero, $D_{3/2}(s)\approx 1$, and $R^{3/2}_{3/2}(s,0)$ amplitude does not get enhanced. Also note that the coefficient of $a_{3/2}$ and $c_{3/2}$ relative to $a_{1/2}$ and $c_{1/2}$ is $1/\sqrt{5}$, which makes it a little less important. Encouraged by these observations, we will approximate

$$R^{3/2}_{3/2}(s,0)\approx 0\,.$$

This assumption, even though very plausible, is somewhat *ad hoc*, for we have not been able to justify it to our satisfaction.

This way, though, we are able to eliminate the the variables $a_{3/2}$ and $c_{3/2}$. Four of the remaining six variables can be eliminated in terms of any two of them. We choose to express everything in terms of c_0 and c_2. First we define the following quantities for shorthand:

$$\gamma = T^{0+}/T^{-+},\quad \eta \equiv \frac{D_0(0)}{D_2(0)}\,\frac{D_2(m_D{}^2)}{D_0(m_D{}^2)}\,,$$

$$\epsilon = [\tfrac{1}{4}(\tfrac{15}{2})^{1/2}(1+\gamma)D_2(m_D{}^2)+\eta(c_2-c_0)]/(1-\eta)\,,$$

$$\beta \equiv (\tfrac{6}{5})^{1/2}[\epsilon + c_2(1-m_\pi{}^2/m_D{}^2)]/D_2(m_\pi{}^2)\,,$$

$$\alpha \equiv \tfrac{1}{2} + \frac{1}{\sqrt{30}}\,[\epsilon(4\eta-1)+4\eta(c_2-c_0)]/D_2(m_D{}^2)\,.$$

Then we can write

$$-if_K R_0{}^{1/2}(s,0) = -\frac{4}{\sqrt{5}}\,\frac{D_0(0)}{D_2(0)}\,\frac{c_2+\epsilon - sc_0/m_D{}^2}{D_0(s)}\,T^{-+}\,,$$

$$-if_K R_2{}^{3/2}(s,0) = \frac{C_2(1-s/m_D{}^2)+\epsilon}{D_2(s)}\,T^{-+}\,,$$

$$if_K R_{1/2}{}^{3/2}(s,0) = \frac{T^{-+}}{D_{1/2}(s)}\left(\alpha D_{1/2}(m_K{}^2) + \frac{m_K{}^2 - s}{m_D{}^2 - m_K{}^2}\left\{\alpha[D_{1/2}(m_K{}^2)+D_{1/2}(m_D{}^2)] - D_{1/2}(m_D{}^2)\left[\beta - \frac{1}{2}\,\frac{f_K}{f_\pi}(1-\gamma)\right]\right\}\right)\,.$$

Clearly, c_0 and c_2, the two free parameters not yet fixed, will take values in the neighborhood of $D_0(m_D{}^2)$ and $D_2(m_D{}^2)$, respectively. Unfortunately, we do not have any more constraints to determined them any better. Instead we choose to vary the values of C_0 and C_2 around the expected numbers and see how the results depend on it.

As explained in Appendix B, the $I=0$ $\pi\pi$ phase shift seems to approach 2π and the corresponding function $D_0(s)$ is determined up to another free parameter. By the help of the computer we studied the behavior of the final answer on these three parameters. We found that the answer does depend on the parameters, and this dependence is rather sensitive. Variations by a factor of 4 in the rate occur as the parameters are allowed to vary over a reasonable range of different values. However, we were encouraged that by choosing the best value we could find for the variables, we obtained

$$\frac{\Gamma(D^+\to K^-\pi^+\pi^+)}{\Gamma(D^0\to K^-\pi^+)}\approx 1.38,\quad \frac{\Gamma(D^0\to \bar{K}^0\pi^+\pi^-)}{\Gamma(D^0\to K^-\pi^+)}\approx 2.12$$

with the following values

$$C_2\approx -0.4,\quad C_0\approx 0.1$$

and the Omnès functions shown in Fig. 3, 4, and 5. The ratios of the rates for other decays are summarised in Table III.

Certainly this answer is much more accurate than we have any right to expect. The weakest thing about it is, of course, its dependence on the choice of the parameters. The underdetermined nature of the problem has forced us to guess the the value of the parameters, and we have shown that there exist values for which the right enhancement is produced and the ratio of the three-body rates to the two-body rates is increased by a factor of 4 to 6 compared to the constant approximation. We admit that this is no proof that the enhancement mentioned is actually produced by the mechanism we suggested. A similar analysis of the other charmed decays, especially that of F^+, may provide examples that are

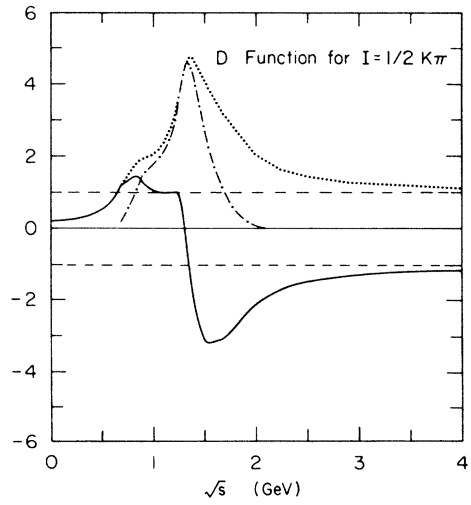

FIG. 3. Numerically computed Omnès function for $I=\frac{1}{2}$ $K\pi$ scattering. The solid, dash-dotted and dotted curves correspond to $\mathrm{Re}[1/D(s)]$, $\mathrm{Im}[1/D(s)]$, and $1/|D(s)|$, respectively.

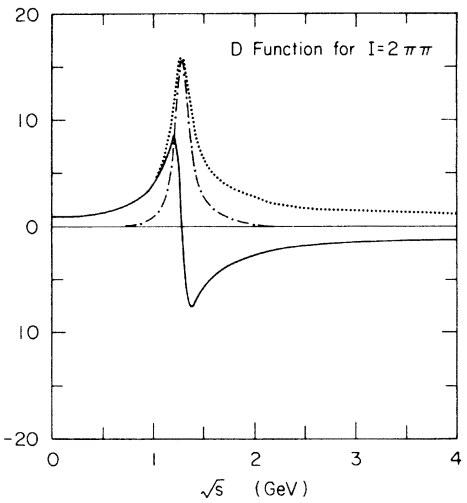

FIG. 4. Numerically computed Omnès function for $I=2$ $\pi\pi$ scattering. The solid dash-dotted and dotted curves correspond to Re$[1/D(s)]$, Im$[1/D(s)]$, and $1/|D(s)|$, respectively.

not overdetermined (or just depending on one parameter only). After such analysis is completed and compared to the forthcoming data on F^+, we hope a better understanding of the problem can be achieved.

III. CONCLUSION

We conclude that the $\Delta I=1$ assumption is a powerful one, and its predictions are summarized in Table II. The preliminary results based on few data indicate a possible disagreement. The experimental rate for the $D^0\to K^-\pi^+\pi^0$ seems to be too large compared to both our prediction and that of Ref. 1.[3] In any case, more data and better statistics are needed to establish this disagreement, if it exists. Such a disagreement may jeopardize the $\Delta I=1$ hypothesis. However, a more likely explanation for a possible disagreement would be the dynamical (by some yet unknown reason) enhancement of the p-wave amplitudes. We must also mention here that the current preliminary experimental rate is not only too high for our s-wave amplitudes, but also for the statistical-model prediction by Quigg and Rosner, in which the p-wave amplitudes are certainly not suppressed.

The question of the three-body final-state enhancement by means of the final-state inter-

TABLE III. The predicted rates for $D\to\bar{K}\pi\pi$ decays with $C_2\approx -0.4$, $C_0\approx 0.1$, and the Omnès functions given in Figs. 3, 4, and 5. All rates are normalized to the $D^0\to K^-\pi^+$ rate.

Decay rate for	Computed relative rate
$(D^0\to K^-\pi^+$	1
$(D^+\to K^-\pi^+\pi^+)$	1.38
$(D^+\to \bar{K}^0\pi^+\pi^0)$	0.35
$(D^0\to \bar{K}^0\pi^+\pi^-)$	2.12
$(D^0\to K^-\pi^+\pi^0)$	0.35
$(D^0\to \bar{K}^0\pi^0\pi^0)$	0.59

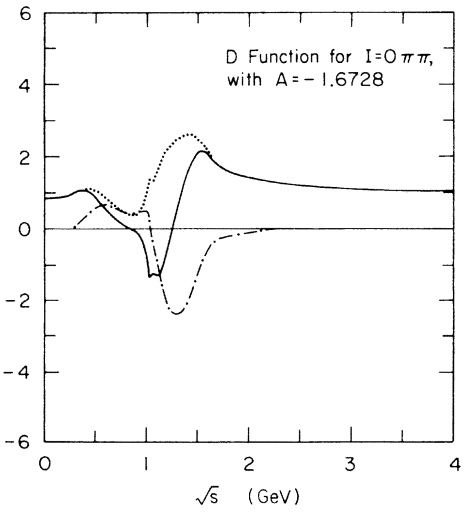

FIG. 5. Numerically computed Omnès function for $I=0$ $\pi\pi$ scattering. The solid, dash-dotted, and dotted curves correspond to Re$[1/D(s)]$, Im$[1/D(s)]$, and $1/|D(s)|$, respectively. The coefficient of s in $Q_2(s)$ is A.

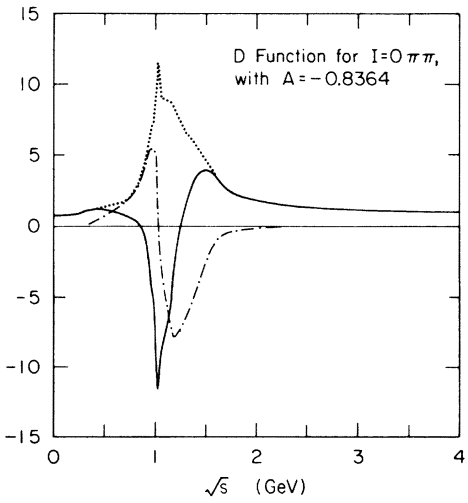

FIG. 6. Numerically computed Omnès function for $I=0$ $\pi\pi$ scattering. The solid, dash-dotted, and dotted curves correspond to Re$[1/D(s)]$, Im$[1/D(s)]$, and $1/|D(s)|$, respectively. The coefficient of s in $Q_2(s)$ is A.

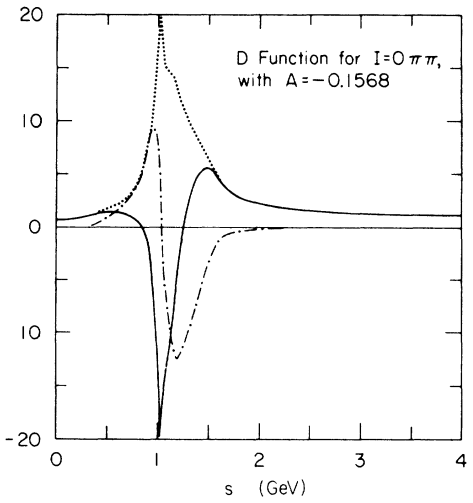

FIG. 7. Numerically computed Omnès function for $I=0$ $\pi\pi$ scattering. The solid, dash-dotted, and dotted curves correspond to Re $[1/D(s)]$, Im $[1/D(s)]$, and $1/|D(s)|$, respectively. The coefficient of s in $Q_2(s)$ is A.

actions may take a lot longer to settle. Certainly, if the $\Delta I=1$ assumption is supported by the data, the manipulation of the final-state interactions becomes easier, and there is hope that F^+ decays may help our understanding. If, however, the $\Delta I=1$ assumption turns out to be incorrect, the enhancement by means of the final-state interactions is still possible and may still be correct; nevertheless, the problem contains very many parameters in this case, and the issue becomes hopelessly complicated and too parameter-dependent for us to deal with.

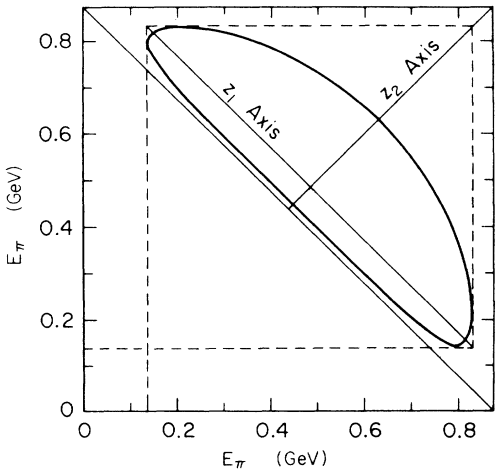

FIG. 8. The allowed energy region for the $D\to\bar{K}\pi\pi$ decay, where the axes correspond to the energies of the final pions. In the following figures the matrix elements are plotted along the z_1 and z_2 axes shown in this figure to demonstrate that the enhancement is achieved without any resonant intermediate states.

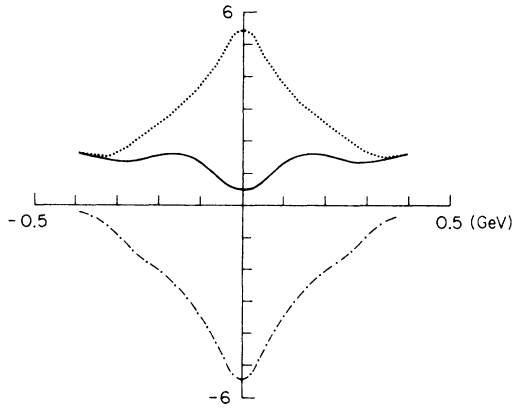

FIG. 9. The matrix element for $D^+\to K^-\pi^+\pi^+$ decay plotted along the z_1 axis. The solid curve is for the real part, the dash-dotted curve is for the imaginary part, and the dotted curve is for the absolute value.

ACKNOWLEDGMENTS

This reasearch was supported by the Department of Energy. I would like to thank James Bjorken for suggesting this problem and numerous invaluable discussions. I would also like to thank F. Gilman for useful discussions.

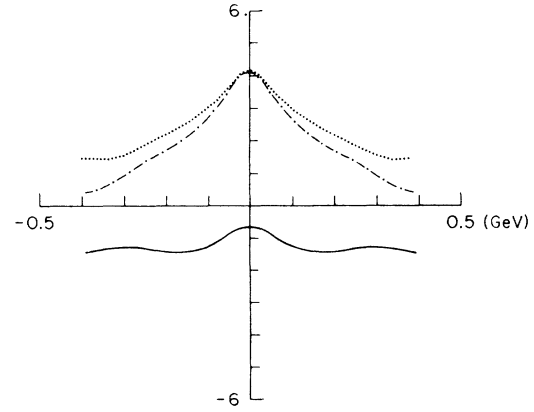

FIG. 10. The matrix element for $D^0\to\bar{K}^0\pi^+\pi^-$ decay plotted along the z_1 axis. The solid curve is for the real part, the dash-dotted curve is for the imaginary part, and the dotted curve is for the absolute value.

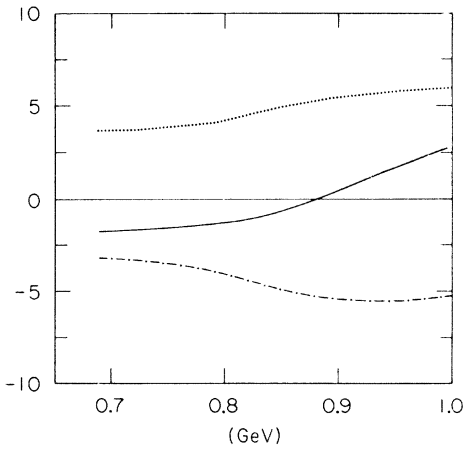

FIG. 11. The matrix element for $D^+ \to K^- \pi^+ \pi^+$ decay plotted along the z_2 axis. The solid curve is for the real part, the dash-dotted curve is for the imaginary part, and the dotted curve is for the absolute value.

APPENDIX A: THE PCAC RELATIONS FOR $D\bar{K}\pi\pi\pi$ DECAYS

1. The pion PCAC relations

Using Eq. (3) we obtain for all $D \to \bar{K}\pi\pi\pi$ decays

$$i\sqrt{2}\, f_\pi \mathfrak{M}^{-++}(k_1, k_2, 0; q) = -T^{-+}(k_1, k_2; q) + T^{0+}(k_1, k_2; q),$$

$$\mathfrak{M}^{-++}(k_1, 0, k_3; q) = \mathfrak{M}^{-++}(k_1, k_3, 0; q),$$

$$i\sqrt{2}\, f_\pi \mathfrak{M}^{0+0}(k_1, k_2, 0; q) = -\sqrt{2}\, T^{0+}(k_1, k_2; q),$$

$$i\sqrt{2}\, f_\pi \mathfrak{M}^{0+0}(k_1, 0, k_3; q) = \sqrt{2}\, T^{0+}(k_1, k_3; q) - T^{00}(k_1, k_3; q),$$

$$i\sqrt{2} f_\pi \mathfrak{M}^{0+-}(k_1, k_2, 0; q) = -T^{0+}(k_1, k_2; q) + T^{-+}(k_1, k_2; q) + \sqrt{2}\, T^{00}(k_1, k_2; q),$$

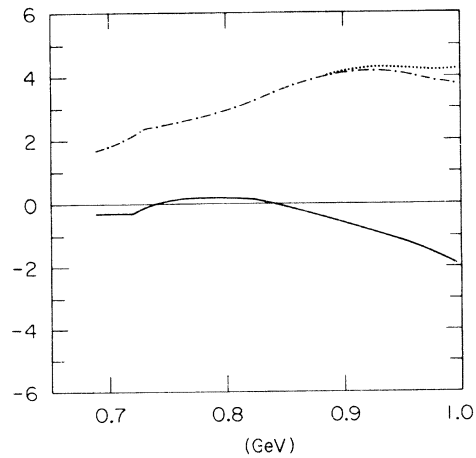

FIG. 12. The matrix element for $D^0 \to \bar{K}^0 \pi^+ \pi^-$ decay plotted along the z_2 axis. The solid curve is for the real part, the dash-dotted cruve is for the imaginary part, and the dotted curve is for the absolute value.

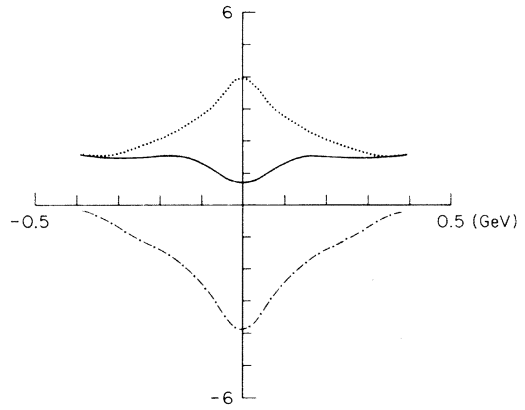

FIG. 13. The matrix element for $D^+ \to K^- \pi^+ \pi^+$ decay plotted along the z_1 axis. The solid curve is for the real part, the dash-dotted curve is for the imaginary part, and the dotted curve is for the absolute value.

$$i\sqrt{2}\, f_\pi \mathfrak{M}^{0+-}(k_1, 0, k_3; q) = -\sqrt{2}\, T^{00}(k_1, k_3; q), \qquad \text{(A1)}$$

$$i\sqrt{2}\, f_\pi \mathfrak{M}^{-+0}(k_1, k_2, 0; q) = -\sqrt{2}\, T^{-+}(k_1, k_2; q),$$

$$i\sqrt{2}\, f_\pi \mathfrak{M}^{-+0}(k_1, 0, k_3; q) = \sqrt{2}\, T^{-+}(k_1, k_3; q) + T^{00}(k_1, k_3; q),$$

$$i\sqrt{2}\, f_\pi \mathfrak{M}^{000}(k_1, k_2, 0; q) = -\sqrt{2}\, T^{00}(k_1, k_2; q),$$

$$\mathfrak{M}^{000}(k_1, 0, k_3; q) = \mathfrak{M}^{000}(k_1, k_3, 0; q),$$

where

$$T^{-+}(k_1, k_2; q) \equiv (K^-(k_1)\pi^+(k_2)|H_w(0)|D^0(p)),$$

$$T^{00}(k_1, k_2; q) \equiv (\bar{K}^0(k_1)\pi^0(k_2)|H_w(0)|D^0(p)),$$

$$T^{0+}(k_1, k_2; q) \equiv (\bar{K}^0(k_1)\pi^+(k_2)|H_w(0)|D^+(p)).$$

Now we symmetrize these amplitudes with respect to the pions

$$\mathfrak{N}^{-++}(k_1, k_2, k_3; q) = \mathfrak{M}^{-++}(k_1, k_2, k_3; q),$$

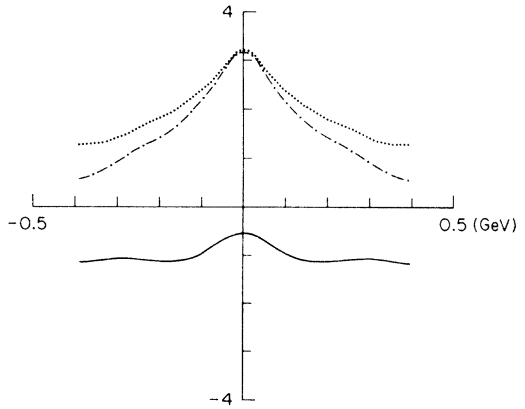

FIG. 14. The matrix element for $D^0 \to \bar{K}^0 \pi^+ \pi^-$ decay plotted along the z_1 axis. The solid curve is for the real part, the dash-dotted curve is for the imaginary part, and the dotted curve is for the absolute value.

$$\sqrt{2}\,\mathfrak{A}^{0+0}(k_1,k_2,k_3;q)=\mathfrak{M}^{0+0}(k_1,k_2,k_3;q)+\mathfrak{M}^{0+0}(k_1,k_3,k_2;q),$$

$$\sqrt{2}\,\mathfrak{A}^{0+-}(k_1,k_2,k;q)=\mathfrak{M}^{0+-}(k_1,k_2,k_3;q)+\mathfrak{M}^{0+-}(k_1,k_3,k_2;q),$$

$$\sqrt{2}\,\mathfrak{A}^{-+0}(k_1,k_2,k_3;q)=\mathfrak{M}^{-+0}(k_1,k_2,k_3;q)+\mathfrak{M}^{-+0}(k_1,k_3,k_2;q),$$

$$\mathfrak{A}^{000}(k_1,k_2,k_3;q)=\mathfrak{M}^{000}(k_1,k_2,k_3;q).$$

Then the PCAC relations can be written as

$$i\sqrt{2}\,f_\pi\,\mathfrak{A}^{-++}(k_1,k_2,0;q)=-T^{-+}(k_1,k_2;q)+T^{0+}(k_1,k_2;q), \tag{A2}$$

$$i\sqrt{2}\,f_\pi\,\mathfrak{A}^{0+0}(k_1,k_2,0;q)=-\frac{1}{\sqrt{2}}\,T^{00}(k_1,k_2;q), \tag{A3}$$

$$i\sqrt{2}\,f_\pi\,\mathfrak{A}^{0+-}(k_1,k_2,0;q)=\frac{1}{\sqrt{2}}\,[T^{-+}(k_1,k_2;q)-T^{0+}(k_1,k_2;q)], \tag{A4}$$

$$i\sqrt{2}\,f_\pi\,\mathfrak{A}^{-+0}(k_1,k_2;q)=\frac{1}{\sqrt{2}}\,T^{00}(k_1,k_2;q), \tag{A5}$$

$$i\sqrt{2}\,f_\pi\,\mathfrak{A}^{000}(k_1,k_2,0;q)=-\sqrt{2}\,T^{00}(k_1,k_2;q). \tag{A6}$$

2. The PCAC relations for both pions taken out simultaneously

The simultaneous treatment of both pions is more complicated than the previous case. The general framework can be found in Ref. 14 or in more detail in Ref. 15. We will merely state the general result applied to the decays of D mesons

$$\mathfrak{M}^{ij}(k_1,0,0;q)=-\frac{i}{2f_{(i)}f_{(j)}}\Big\{(K(k_1)|[Q^j,[Q^i,H_w]]|D(p))+(\bar K(k_1)|[Q^i,[Q^j,H_w]]|D(p))$$
$$-f_{(i)}m_\pi^2\int d^4x\,(\bar K(k_1)|T[\sigma^{ji}(x)H_w(0)]|D(p))$$
$$-f_{(j)}m_\pi^2\int d^4x(\bar K(k_1)|T[\sigma^{ij}(x)H_w(0)]|D(p))\Big\}.$$

We will neglect the σ terms since they are proportional to the squared pion mass. Then for individual amplitudes we get

$$f_\pi^2\mathfrak{M}^{-++}(k_1,0,0;q)=(\bar K^0(k_1)|H_w(0)|D^0(p)),$$

$$f_\pi^2\mathfrak{M}^{0+0}(k_1,0,0;q)=-\frac{1}{2\sqrt{2}}(\bar K^0(k_1)|H_w(0)|D^0(p)),$$

$$f_\pi^2\mathfrak{M}^{0+-}(k_1,0,0;q)=-\tfrac{1}{2}(\bar K^0(k_1)|H_w(0)|D^0(p)),$$

$$f_\pi^2\mathfrak{M}^{-+0}(k_1,0,0;q)=\frac{1}{2\sqrt{2}}(\bar K^0(k_1)|H_w(0)|D^0(p)),$$

$$f_\pi^2\mathfrak{M}^{000}(k_1,0,0;q)=-(\bar K^0(k_1)|H_w(0)|D^0(p)).$$

After symmetrization this can be written as

$$\mathfrak{A}^{0+0}(k_1,0,0;q)=-\tfrac{1}{2}\mathfrak{A}^{-++}(k_1,0,0;q), \tag{A7}$$

$$\mathfrak{A}^{0+-}(k_1,0,0;q)=-\frac{1}{\sqrt{2}}\mathfrak{A}^{-++}(k_1,0,0;q), \tag{A8}$$

$$\mathfrak{A}^{-+0}(k_1,0,0;q)=\tfrac{1}{2}\mathfrak{A}^{-++}(k_1,0,0;q), \tag{A9}$$

$$\mathfrak{A}^{000}(k_1,0,0;q)=-\mathfrak{A}^{-++}(k_1,0,0;q). \tag{A10}$$

As we see here, PCAC strongly suggests the $\Delta I=1$ hypothesis. Actually with the $\Delta I=1$ assumption, Eqs. (A7) and (A9) become trivial.

3. Kaon PCAC relations

As in Sec. (A), we immediately obtain

$$if_K\,\mathfrak{A}^{0+-}(0,k_2,k_3;q)=-\tfrac{1}{2}(T^{-+}(k_2,k_3;q)+T^{-+}(k_3,k_2;q)), \tag{A11}$$

$$if_K\,\mathfrak{A}^{000}(0,k_2,k_3;q)=\tfrac{1}{2}(T^{00}(k_2,k_3;q)+T^{00}(k_3,k_2;q)), \tag{A12}$$

$$if_K\,\mathfrak{A}^{-++}(0,k_2,k_3;q)=-\frac{1}{\sqrt{2}}(T^{0+}(k_2,k_3;q)+T^{0+}(k_3,k_2;q)). \tag{A13}$$

Note that only two of these equations are independent. When substituted into Eqs. (28) and (29), they yield

$$T^{-+}-T^{0+}+\sqrt{2}\,T^{00}=0,$$

which is identical to Eq. (8).

APPENDIX B: FINAL-STATE INTERACTIONS AND OMNÈS FUNCTIONS

For a good review of this subject and an extensive list of references, see Basdevant.[16]

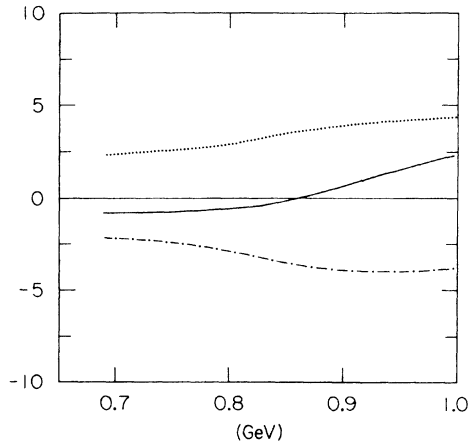

FIG. 15. The matrix element for $D^+ \to K^-\pi^+\pi^+$ decay plotted along the z_2 axis. The solid curve is for the real part, the dash-dotted curve is for the imaginary part, and the dotted curve is for the absolute value.

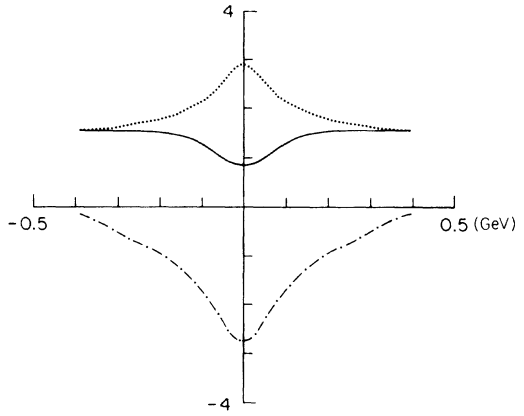

FIG. 17. The matrix element for $D^+ \to K^-\pi^+\pi^+$ decay plotted along the z_1 axis. The solid curve is for the real part, the dash-dotted curve is for the imaginary part, and the dotted curve is for the absolute value.

1. Omnès functions

Suppose we would like to find an analytic function $A(s)$ in the complex s plane cut along the real axis from s_0 to $+\infty$, such that

(i) the phase of $A(s+i\epsilon)$ is a known function $\delta(s)$ as $\epsilon \to 0^+$ along the cut,

(ii) $A(s)$ is real on an open interval on the real axis that lies to the left of the point s_0,

(iii) $A(s_0)=1$,

(iv) $\lim_{s\to\infty} |A(s)| = 1$.

For real s, it turns out that the solution can be written as

$$A(s) = \frac{Q_m(s)}{|s-s_0|^m}\, e^{i\delta(s)\phi(s-s_0)} \times \exp\left\{\frac{1}{\pi}\lim_{\epsilon\to 0^+}\int_{s_0}^{\infty}[\delta(s')-m\pi]\,\frac{(s'-s)\,ds'}{(s'-s)^2+\epsilon^2}\right\},$$

where $Q_m(s)$ is a polynomial of degree $m \in N$ with unit leading coefficient. Other coefficients in $Q_m(s)$ must be fixed such that $A(s_0)=1$. For analyticity we also have to have $m = \lim_{s\to\infty}(s)/\pi$. Without this condition the problem cannot be solved.

We will define

$$D(s) = 1/A(s).$$

For $K\pi$ scattering, $\lim_{s\to\infty}\delta^{1/2}(s) = \pi$; hence $D_{1/2}(s)$ is fully determined. The same is true

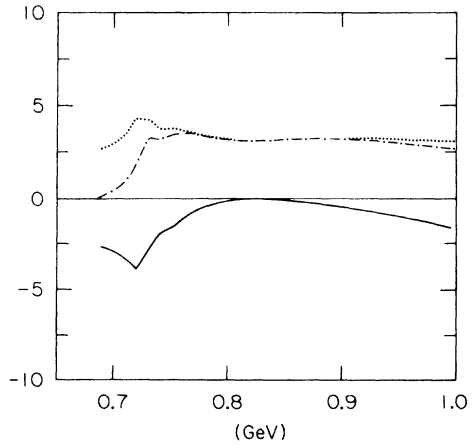

FIG. 16. The matrix element for $D^0 \to \bar{K}^0\pi^+\pi^-$ decay plotted along the z_2 axis. The solid curve is for the real part, the dash-dotted curve is for the imaginary part, and the dotted curve is for the absolute value.

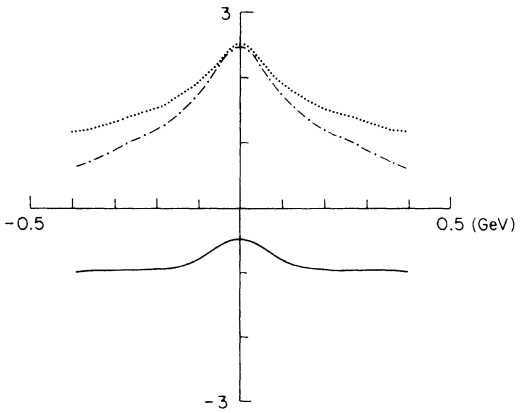

FIG. 18. The matrix element for $D^0 \to \bar{K}^0\pi^+\pi^-$ decay plotted along the z_1 axis. The solid curve is for the real part, the dash-dotted curve is for the imaginary part, and the dotted curve is for the absolute value.

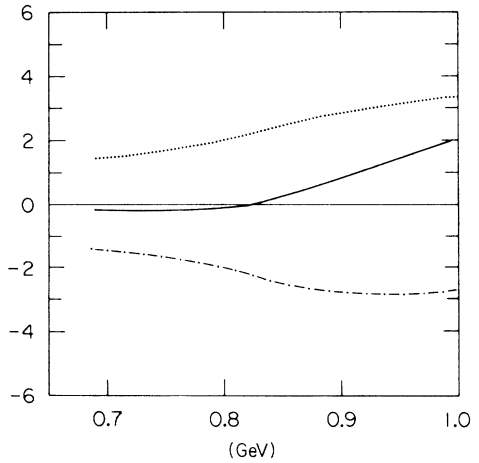

FIG. 19. The matrix element for $D^+ \to K^- \pi^+ \pi^+$ decay plotted along the z_2 axis. The solid curve is for the real part, the dash-dotted curve is for the imaginary part, and the dotted curve is for the absolute value.

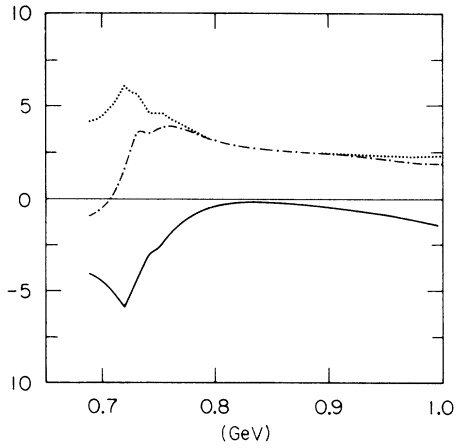

FIG. 20. The matrix element for $D^0 \to \bar{K}^0 \pi^+ \pi^-$ decay plotted along the z_2 axis. The solid curve is for the real part, the dash-dotted curve is for the imaginary part, and the dotted curve is for the absolute value.

for $I=2$ $\pi\pi$ scattering and $D_2(s)$. For $I=0$ $\pi\pi$ scattering, however, $\lim_{s\to\infty} \delta^0(s) = 2\pi$ and $Q_2(s)$ is not uniquely fixed by the requirement $A(s_0)=1$. The $I=\frac{3}{2}$ part of $K\pi$ scattering is trivial since $\delta^{3/2}(s) \approx 0$; hence $D_{3/2}(s) \approx 1$. In all of these applications, s_0 is the invariant mass squared at the threshold.

2. Elastic and inelastic scattering

Consider the $D \to \bar{K}\pi$, $D \to \pi\pi$, and $D \to K\bar{K}$ amplitudes. Separating the isospin parts and using unitarity we immediately obtain for the $I=2$ and $I=\frac{3}{2}$ $D \to \bar{K}\pi$ decay amplitudes

$$T_{1/2} \cong |T_{1/2}| \exp[i\delta^{1/2}(s)],$$

$$T_{3/2} \cong |T_{3/2}| \exp[i\delta^{3/2}(s)].$$

Therefore, $T_{1/2}$ and $T_{3/2}$ are given by the inverse of the corresponding Onmès functions. $I=2$ $D \to \pi\pi$ gives similarly

$$T_2 \cong |T_2| \exp[i\delta^2(s)].$$

However, $I=0$ $\pi\pi$ or $K\bar{K}$ final state is fairly inelastic, especially around S^*. The transition $\pi\pi \to K\bar{K}$ can proceed strongly. In this case the transition amplitude is

$$\mathfrak{U} \cong (1-\eta^2)^{1/2} \exp[i(\delta^0_{\pi\pi} + \delta^0_{K\bar{K}})].$$

Writing

$$T_0^{\pi\pi} = |T_0| e^{i\phi},$$

$$T_0^{K\bar{K}} = |T_0'| e^{i\phi'},$$

we obtain

$$[\eta - e^{2i(\phi - \delta^0_{\pi\pi})}][\eta - e^{2i(\phi' - \delta^0_{K\bar{K}})}] = 1 - \eta^2,$$

which has solutions

$$\phi = \delta^0_{\pi\pi} \mp \tfrac{1}{2} \arccos(\eta),$$

$$\phi' = \delta^0_{K\bar{K}} \pm \tfrac{1}{2} \arccos(\eta).$$

Therefore, even in the inelastic case it is possible to define a modified Omnès function by redefining the phase shift. For our approximate treatment of the $D \to \bar{K}\pi\pi$ decay the usage of this effective phase shift will suffice, and we will not attempt to treat the inelastic problem with any more rigor than this.

3. Three-body final states

The general treatment is very difficult, and it is never used in this paper. The treatment of the case where particles interact two at a time, but never all three together, can be reduced to the linear approximation in terms of the two-particle amplitudes we used.

4. Actual Omnès functions for $I = 1/2$ $K\pi$, $I = 2$ $\pi\pi$, and $I = 0$ $\pi\pi$ scattering

Using the known phase shifts and the $\pi\pi$ inelasticity for $I=0$, we produced the graphs given in Fig. 3 through 7 by means of numerical integration. The best values for the enhancement of $D \to \bar{K}\pi\pi$ decays involve Fig. 5 for $I=0$ $\pi\pi$ scattering. In Fig. 9–20 we plotted the variation of the full matrix element on the selected axes shown in Fig. 8 to exhibit the enhancement without any resonant intermediate states.

*Address after Sept. 1, 1978: Institute for Theoretical Physics, State University of New York at Stony Brook, Stony Brook, N. Y. 11794.

[1]G. Goldhaber *et al.*, Phys. Rev. Lett. 37, 225 (1976); I. Peruzzi *et al.*, *ibid.* 37, 569 (1976).

[2]R. Brandelik *et al.*, Phys. Lett. 70B, 132 (1977); S. Yamada, in *Proceedings of the International Symposium on Lepton and Photon Interactions at High Energies, Hamburg, 1977*, edited by F. Gutbrod (DESY, Hamburg, 1977).

[3]In addition, while this paper was being prepared, the SLAC-LBL group observed a signal coming from the $D^0 \to K^- \pi^- \pi^0$ decay. See D. L. Scharre *et al.*, Phys. Rev. Lett. 40, 74 (1978).

[4]W. Braunschweig *et al.*, Phys. Lett. 63B, 471 (1976); J. L. Burmester *et al.*, *ibid.* 64B, 369 (1976).

[5]H. K. Nguyen *et al.*, Phys. Rev. Lett. 37, 1531 (1976).

[6]J. D. Bjorken and S. L. Glashow, Phys. Lett. 11, 225 (1964).

[7]M. Piccolo *et al.*, Phys. Lett. 70B, 260 (1977).

[8]G. J. Feldman, SLAC Report No. SLAC-PUB-2000 [invited talk at SLAC Summer Institute on Particle Physics, 1977, Stanford (unpublished)].

[9]M. K. Gaillard, B. W. Lee, and J. L. Rosner, Rev. Mod. Phys. 47, 227 (1975).

[10]J. D. Jackson, in *Proceedings of Summer Institute on Particle Physics, Stanford, 1976*, edited by Martha C. Zipf (SLAC, Stanford, 1976).

[11]C. Quigg and J. L. Rosner, Phys. Rev. D 17, 239 (1978).

[12]M. Suzuki, Phys. Rev. 144, 1154 (1966); S. K. Bose, and S. N. Biswas, Phys. Rev. Lett. 16, 346 (1966); J. Weyers, L. L. Foldy, and D. R. Speiser, *ibid.* 17, 1062 (1966); C. G. Callan and S. B. Treiman, *ibid.* 16, 153 (1966); D. K. Elias and J. C. Taylor, Nuovo Cimento 44A, 518 (1966).

[13]R. Omnes, Nuovo Cimento 8, 316 (1958); N. R. Muskhelishvili, *Singular Integral Equations* (Noordhoff, Grogingen, 1953); V. Allessandrini, and R. Omnès, Phys. Rev. 139B, 167 (1965).

[14]Steven Weinberg, Phys. Rev. Lett. 17, 336 (1966).

[15]Robert E. Marshak, Riazuddin, and Ciaran P. Ryan, *Theory of Weak Interactions in Particle Physics* (Wiley, New York, 1969).

[16]J. L. Basdevant, in *Proceedings of the International School of Elementary Particle Physics, Herceg-Novi, Yugoslavia, 1968*, edited by M. Nikolič (Gordon and Breach, New York, 1970).

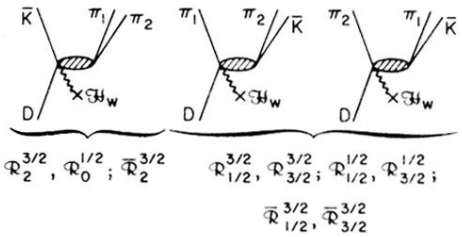

FIG. 1. Approximate form of the three-body amplitude assuming that the final particles interact two at a time, but not all three together.

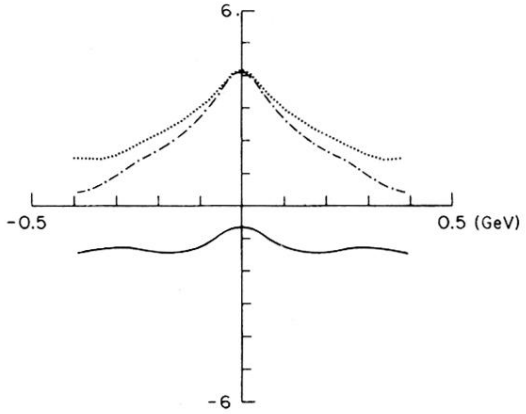

FIG. 10. The matrix element for $D^0 \to \bar{K}^0 \pi^+ \pi^-$ decay plotted along the z_1 axis. The solid curve is for the real part, the dash-dotted curve is for the imaginary part, and the dotted curve is for the absolute value.

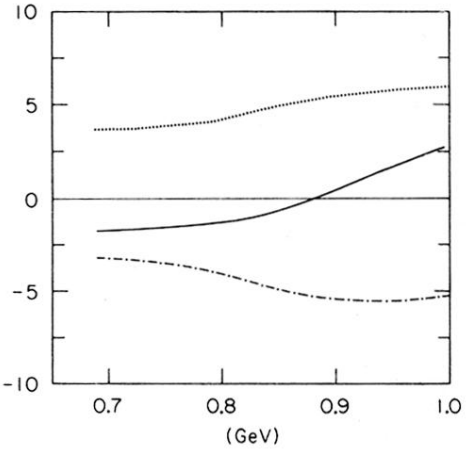

FIG. 11. The matrix element for $D^+ \to K^- \pi^+ \pi^+$ decay plotted along the z_2 axis. The solid curve is for the real part, the dash-dotted curve is for the imaginary part, and the dotted curve is for the absolute value.

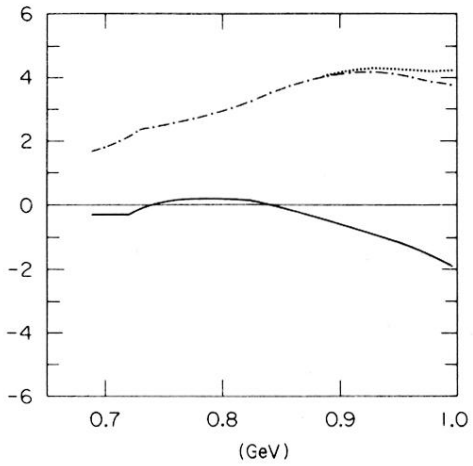

FIG. 12. The matrix element for $D^0 \to \bar{K}^0 \pi^+ \pi^-$ decay plotted along the z_2 axis. The solid curve is for the real part, the dash-dotted cruve is for the imaginary part, and the dotted curve is for the absolute value.

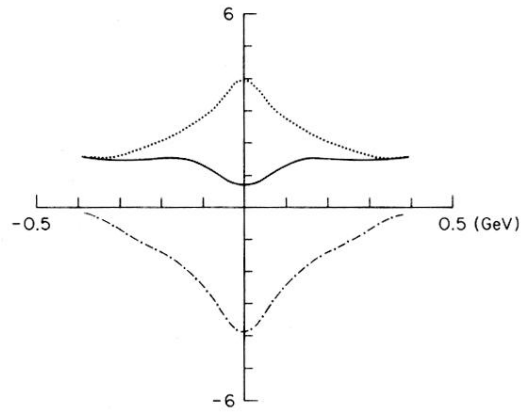

FIG. 13. The matrix element for $D^+ \to K^- \pi^+ \pi^+$ decay plotted along the z_1 axis. The solid curve is for the real part, the dash-dotted curve is for the imaginary part, and the dotted curve is for the absolute value.

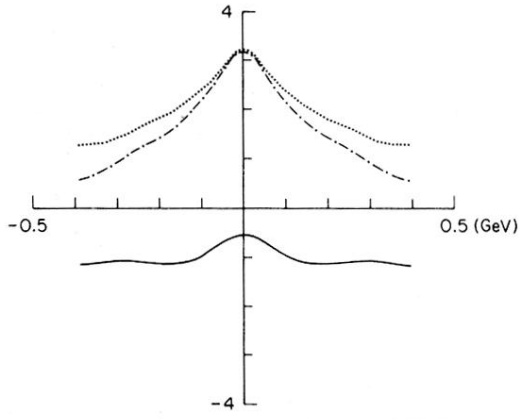

FIG. 14. The matrix element for $D^0 \to \overline{K}^0 \pi^+ \pi^-$ decay plotted along the z_1 axis. The solid curve is for the real part, the dash-dotted curve is for the imaginary part, and the dotted curve is for the absolute value.

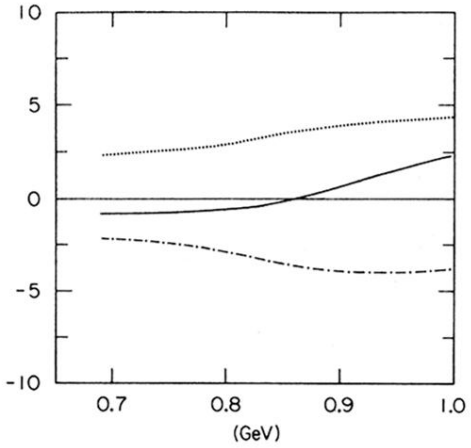

FIG. 15. The matrix element for $D^+ \to K^- \pi^+ \pi^+$ decay plotted along the z_2 axis. The solid curve is for the real part, the dash-dotted curve is for the imaginary part, and the dotted curve is for the absolute value.

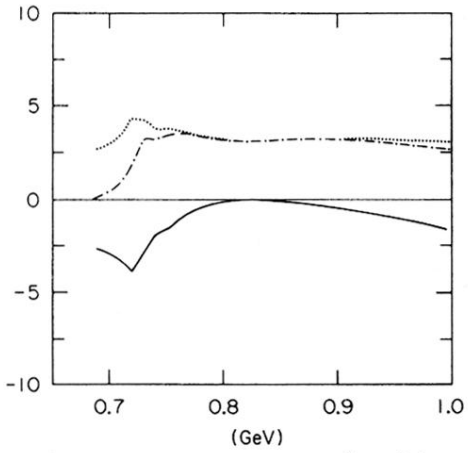

FIG. 16. The matrix element for $D^0 \to \bar{K}^0 \pi^+ \pi^-$ decay plotted along the z_2 axis. The solid curve is for the real part, the dash-dotted curve is for the imaginary part, and the dotted curve is for the absolute value.

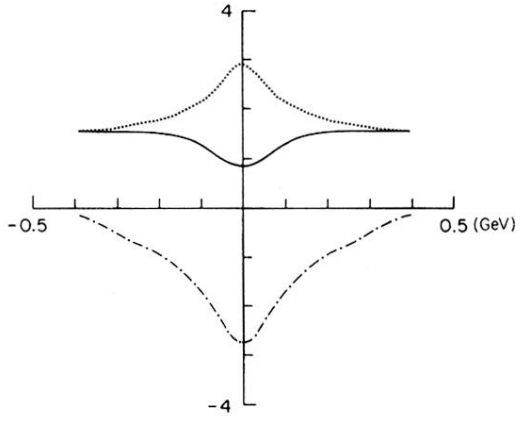

FIG. 17. The matrix element for $D^+ \to K^- \pi^+ \pi^+$ decay plotted along the z_1 axis. The solid curve is for the real part, the dash-dotted curve is for the imaginary part, and the dotted curve is for the absolute value.

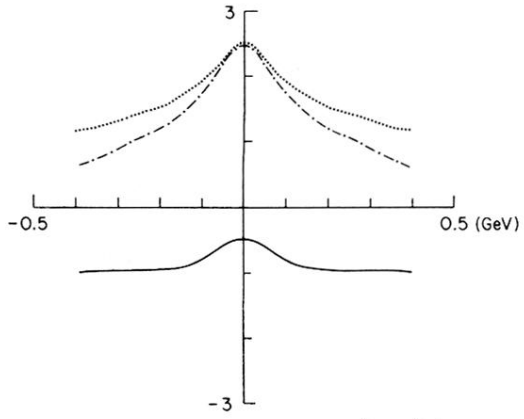

FIG. 18. The matrix element for $D^0 \to \bar{K}^0 \pi^+ \pi^-$ decay plotted along the z_1 axis. The solid curve is for the real part, the dash-dotted curve is for the imaginary part, and the dotted curve is for the absolute value.

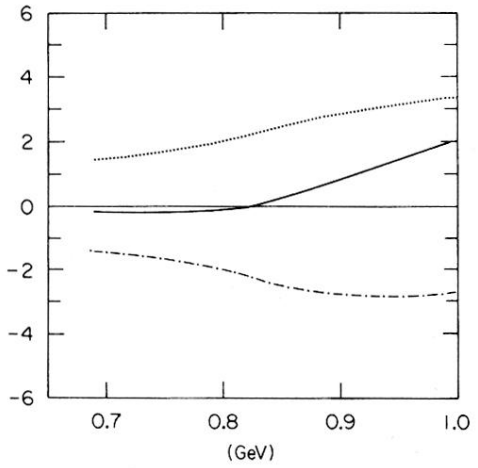

FIG. 19. The matrix element for $D^+ \to K^- \pi^+ \pi^+$ decay plotted along the z_2 axis. The solid curve is for the real part, the dash-dotted curve is for the imaginary part, and the dotted curve is for the absolute value.

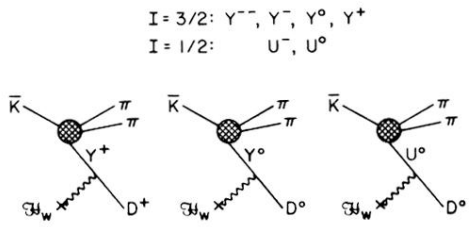

FIG. 2. Equations (22) through (24) can be deduced by assuming the reaction proceeds through the imaginary intermediate states Y and U.

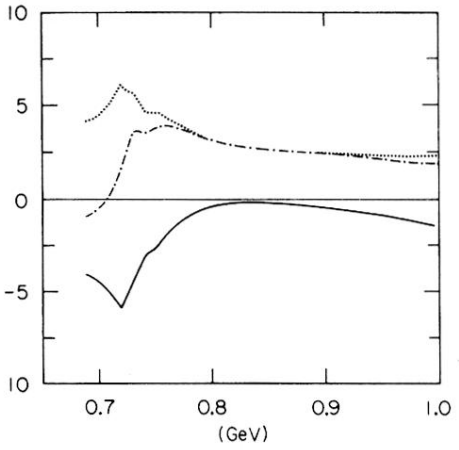

FIG. 20. The matrix element for $D^0 \to \bar{K}^0 \pi^+ \pi^-$ decay plotted along the z_2 axis. The solid curve is for the real part, the dash-dotted curve is for the imaginary part, and the dotted curve is for the absolute value.

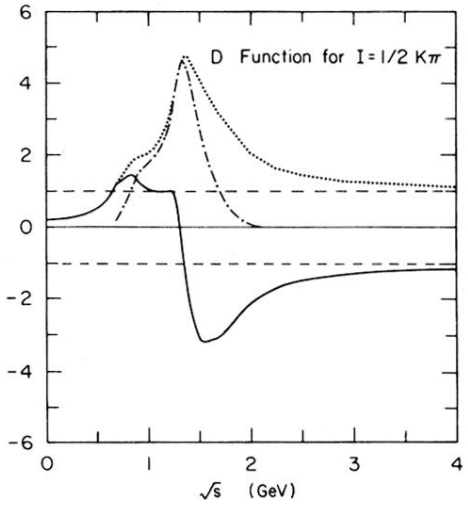

FIG. 3. Numerically computed Omnès function for $I=\frac{1}{2}$ $K\pi$ scattering. The solid, dash-dotted and dotted curves correspond to $\mathrm{Re}[1/D(s)]$, $\mathrm{Im}[1/D(s)]$, and $1/|D(s)|$, respectively.

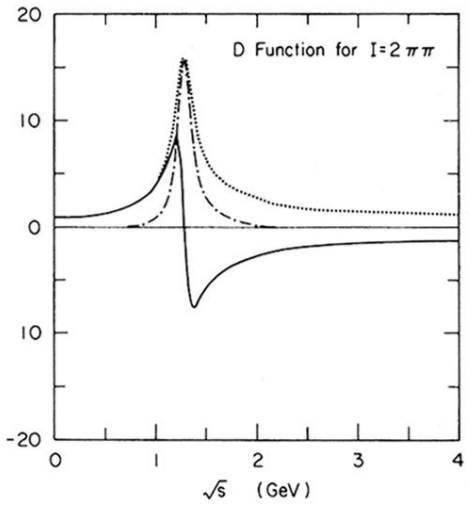

FIG. 4. Numerically computed Omnès function for $I=2\ \pi\pi$ scattering. The solid dash-dotted and dotted curves correspond to Re $[1/D(s)]$, Im $[1/D(s)]$, and $1/|D(s)|$, respectively.

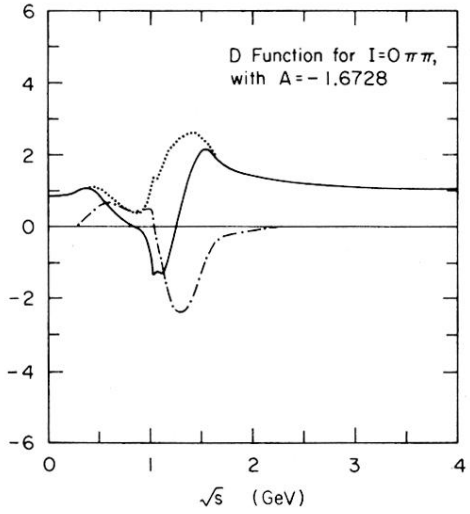

FIG. 5. Numerically computed Omnès function for $I = 0$ $\pi\pi$ scattering. The solid, dash-dotted, and dotted curves correspond to Re $[1/D(s)]$, Im $[1/D(s)]$, and $1/|D(s)|$, respectively. The coefficient of s in $Q_2(s)$ is A.

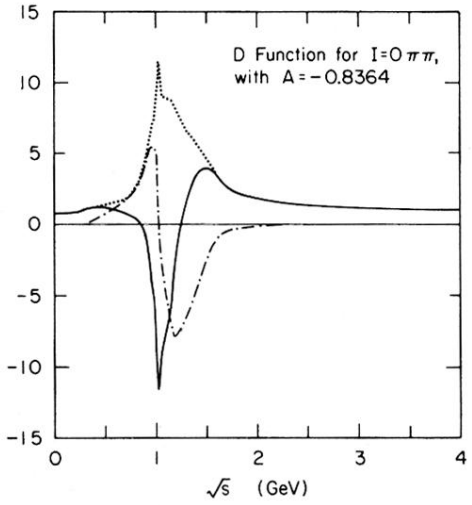

FIG. 6. Numerically computed Omnès function for $I=0$ $\pi\pi$ scattering. The solid, dash-dotted, and dotted curves correspond to Re $[1/D(s)]$, Im $[1/D(s)]$, and $1/|D(s)|$, respectively. The coefficient of s in $Q_2(s)$ is A.

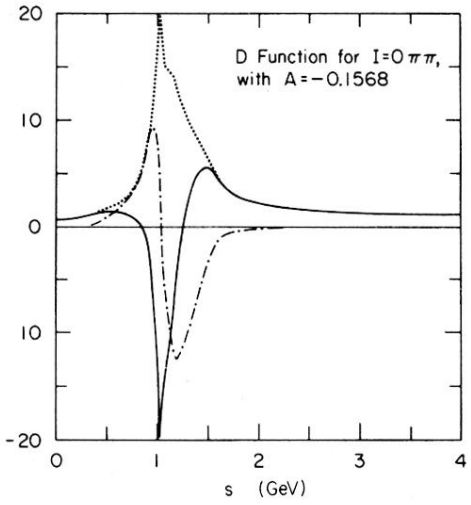

FIG. 7. Numerically computed Omnès function for $I=0$ $\pi\pi$ scattering. The solid, dash-dotted, and dotted curves correspond to Re $[1/D(s)]$, Im $[1/D(s)]$, and $1/|D(s)|$, respectively. The coefficient of s in $Q_2(s)$ is A.

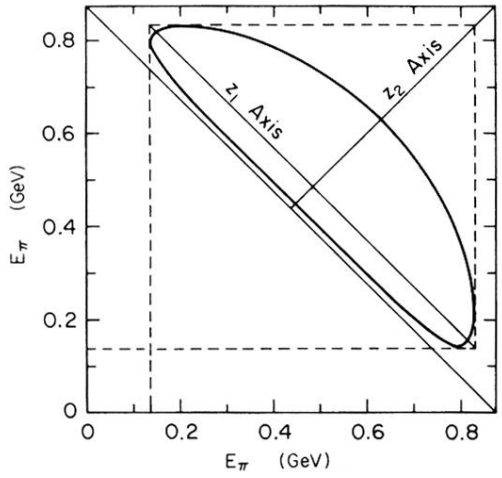

FIG. 8. The allowed energy region for the $D \to \bar{K}\pi\pi$ decay, where the axes correspond to the energies of the final pions. In the following figures the matrix elements are plotted along the z_1 and z_2 axes shown in this figure to demonstrate that the enhancement is achieved without any resonant intermediate states.

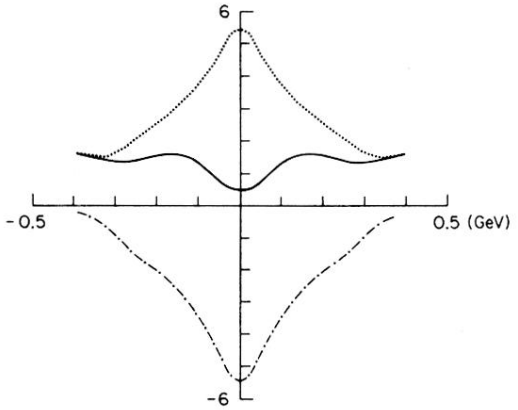

FIG. 9. The matrix element for $D^+ \to K^- \pi^+ \pi^+$ decay plotted along the z_1 axis. The solid curve is for the real part, the dash-dotted curve is for the imaginary part, and the dotted curve is for the absolute value.